# Microscopic calculation of the dynamic structure function in the deep-inelastic regime

A. Belić and V. R. Pandharipande
*Department of Physics, University of Illinois at Urbana-Champaign, 1110 West Green Street, Urbana, Illinois 61801*
(Received 18 July 1990; revised manuscript received 15 May 1991)

We study the dynamic structure function $S(\mathbf{k},\omega)$ of Bose liquids in the asymptotic limit $k,\omega\to\infty$ at constant $y\equiv(m/k)(\omega-k^2/2m)$, using the orthogonal correlated basis of Feynman phonon states. This approach has been traditionally and successfully used to study the $S(\mathbf{k},\omega)$ at small $k,\omega$, and it appears possible to develop it further to obtain a unified theory of $S(\mathbf{k},\omega)$ at all $k$ and $\omega$. In the present work, we prove within this approach that the $S(\mathbf{k},\omega)$ scales exactly in the $k,\omega\to\infty$ limit, as is well known. We also show that, within a very good approximation, the scaling function $J(y)$ is determined solely by the static structure function $S(q)$ of the liquid. In contrast, the traditional approach to the $S(k,\omega)$ at large $k,\omega$ is based on the impulse approximation (IA), and the $J_{\rm IA}(y)$ is solely determined by the momentum distribution $n(q)$ of the particles in the liquid. In weakly interacting systems, where the IA is exact, we show that the $J(y)$ calculated from the Feynman phonon basis is identical to the $J_{\rm IA}(y)$. The theory is applied to liquid $^4$He and the $J(y)$ is calculated using the experimental $S(q)$. This $J(y)$ is quite similar to the $J_{\rm IA}(y)$ obtained from the theoretical $n(q)$ of liquid $^4$He. A number of technical developments in orthogonal-correlated-basis theories are reported.

## I. INTRODUCTION

Deep-inelastic neutron-scattering (DINS) experiments[1–7] measure the dynamic structure function (DSF) $S(\mathbf{k},\omega)$ at large values of $k$ and $\omega$. In this region it has been observed that the DSF exhibits approximate scaling:

$$\frac{k}{m}S(\mathbf{k},\omega)\to J(y),\quad k,\omega\to\infty\ ,$$
$$\text{at } y\equiv\frac{m}{k}\left[\omega-\frac{k^2}{2m}\right]=\text{const}\ , \tag{1.1}$$

where $y$ is the West scaling variable,[8] $m$ the mass of the atom, and $J(y)$ the scaling function. When the interatomic potential is finite the $J(y)$ is given by the impulse approximation[9] (IA) as

$$J_{\rm IA}(y)=\frac{1}{4\pi^2\rho}\int_{|y|}^{\infty}dq\,qn(q)\ , \tag{1.2}$$

where $\rho$ is the density and $n(q)$ is the momentum distribution of the atoms in the system. In this case the struck atom recoils as if it was free, since potential can be neglected when the energy of the atom $\omega$ is large enough. If the same was true for systems with hard-core interaction, like helium liquids, it would be possible to extract their $n(q)$ directly from DINS experiments. However, it has been argued that in this case IA has to be corrected to take into account the fact that the potential is not small with respect to the energy of the struck atom for all $k$ and $\omega$ of practical interest, so that the recoil is not quasi-free. These corrections are known as the final-state-interaction (FSI) effects.

There have been several attempts to calculate the effect of FSI on DSF. In one approach the DSF is written as a convolution of $S_{\rm IA}(\mathbf{k},\omega)$ obtained with the IA and a folding function $F$ as follows:

$$S(\mathbf{k},\omega)=\int d\omega'\,F(k,\omega-\omega')S_{\rm IA}(\mathbf{k},\omega')\ , \tag{1.3}$$

$$F(k,\omega-\omega')=\frac{1}{\pi}\mathrm{Re}\int_0^{\infty}dt\,e^{i(\omega-\omega')t}A(k,t)\ . \tag{1.4}$$

Here $|A(k,t)|^2$ is the probability that the struck atom is in the same momentum state $\mathbf{k}+\mathbf{p}_{\rm initial}$ at time $t$ after the collision with the neutron. More formally, $A(k,t)$ is given by

$$A(k,t)=\frac{\langle 0|\rho_{\mathbf{k}}e^{-iHt}\rho_{\mathbf{k}}^{\dagger}|0\rangle}{\langle 0|\rho_{\mathbf{k}}e^{-iH_0t}\rho_{\mathbf{k}}^{\dagger}|0\rangle}\ , \tag{1.5}$$

where

$$\rho_{\mathbf{k}}=\frac{1}{\sqrt{N}}\sum_j e^{-i\mathbf{k}\cdot\mathbf{r}_j}\ , \tag{1.6}$$

$N$ is the total number of particles, $H_0$ is given by

$$H_0=\sum_i\frac{\mathbf{p}_i^2}{2m}+\sum_{i<j\neq I}v_{ij}\ , \tag{1.7}$$

and $I$ is the index of the struck atom. It is difficult to calculate the $A(k,t)$ and thus the folding function $F(k,\omega-\omega')$ exactly. A number of approximate schemes[9–11] have been developed, and the one developed by Silver and collaborators[12] is quite successful in explaining available data[13] at $k\sim 23$ Å$^{-1}$ on liquid $^4$He. Monte Carlo calculations[14] of the folding function have also been quite successful at $k\sim 10$ and 23 Å$^{-1}$.

In another approach the $S(\mathbf{k},\omega)$ at large $k$ and $\omega$ is expanded in powers of $m/k$:

$$\frac{k}{m}S(\mathbf{k},\omega)=J(y)+\frac{m}{k}J_1(y)+\left[\frac{m}{k}\right]^2J_2(y)+\cdots\ . \tag{1.8}$$

The $\omega^n$ weighted moments of DSF can be related to the

 

$y^n$ moments of $J_m(y)$ if the ground-state wave function is known, using the relation[15]

$$\int_0^\infty d\omega\, \omega^n S(\mathbf{k},\omega)=\langle 0|\rho_{\mathbf{k}}[H,\ldots,[H,\rho_{\mathbf{k}}^\dagger]\ldots]|0\rangle\ , \quad (1.9)$$

where there are $n$ commutators in the expectation value. In particular it has been shown[16,17] that

$$\int_{-k/2}^\infty dy\, y^n J(y)=\int_{-k/2}^\infty dy\, y^n J_{\mathrm{IA}}(y)=\frac{\langle 0|p_i^n|0\rangle}{n+1} \quad (1.10)$$

for all values of $n$. This observation implies that the asymptotic $J(y)$ is given by $J_{\mathrm{IA}}(y)$, and effects of FSI are of order $m/k$.

The moments of other $J_m(y)$ can also be calculated; for example,[18]

$$\int_{-k/2}^\infty dy\, y^n J_1(y) =(-1)^{(n+1)/2}\sum_{m=1}^{n-1}(n-m)\begin{pmatrix} n \\ m-1 \end{pmatrix} \times \sum_{j(\neq i)}\langle 0|[\partial_{z,i}^{n-m}v(r_{ij})]\partial_{z,i}^{m-1}|0\rangle\ . \quad (1.11)$$

It is, however, difficult to obtain an expression for $J_1(y)$ which will satisfy all these moments. In practice, only first few moments are calculated, and the $J_1(y)$ is estimated from these by using an orthogonal polynomial expansion. The results of such studies are in qualitative agreement with the experimental data on liquid $^4$He.[18]

If the interatomic potential is finite, the $J_n(y)$ can be computed[19] in terms of many-body distribution functions. For example, $J_1(y)$ can be evaluated using the off-diagonal two-body density matrix $\rho_2$:

$$J_1(y)=-\frac{1}{2\pi\rho}\int_{-\infty}^\infty ds\, e^{iys}\int d^3r\,\rho_2(\mathbf{r}-s\hat{\mathbf{k}},0,\mathbf{r},0) \times\int_0^s du[v(\mathbf{r}-u\hat{\mathbf{k}})-v(\mathbf{r})]\ . \quad (1.12)$$

Unfortunately these formulas do not apply to the hard core systems. The $u$ integral in the above expression is divergent when path of integration passes through the hard core region. A remedy for this problem may be to use the $T$ matrix instead of the bare potential[20,21] to calculate functions $J_n(y)$. However, these functions then become $k$ dependent because the $T$ matrix is $k$ dependent and the simple expansion (1.8) is invalidated.

In the limit $k\to\infty,\omega\to\infty$ at constant $y$, it has been proved that $S(\mathbf{k},\omega)$ is a function of $y$ alone.[22] However, the $J(y)$ for Bose hard sphere gas obtained by summing a selected class of terms using the many-body perturbation theory developed by Brueckner, Bethe, and Goldstone gave an asymptotic $J(y)$ different from the $J_{\mathrm{IA}}(y)$.

All the theories mentioned above, with the exception of Ref. 22, start from the IA that takes into account the interactions in the initial state of the target, and try to improve upon it by incorporating the effects of FSI. This procedure gets more and more difficult as $k$ decreases and the FSI effects become more important. In contrast the response at small $k$ and $\omega$ is easily treated by using Feynman phonon states.[15] In particular the orthogonal correlated basis formalism[23] based on Feynman's ideas is quite successful in explaining the observed $S(\mathbf{k},\omega)$ at $k\lesssim 2$ Å$^{-1}$. The small and large $k$ methods have different starting points; the momentum distribution $n(q)$ is the main input for the IA, while the OCB formalism uses the static structure function $S(q)$ as the main input. The $S(q)$ and $n(q)$ are not unrelated. For example, if one uses the Jastrow wave function

$$\Psi_J=\prod_{i<j}f_J(r_{ij}) \quad (1.13)$$

to approximate the ground state, then the $S(q)$ [i.e., the pair distribution function $g(r)$] determines[14,15] $f_J(r)$ and hence $n(q)$. However, it is not clear that there exists a one-to-one correspondence between the $S(q)$ and $n(q)$ of a general Bose ground-state wave function.

In principle the OCB formalism can be used to study $S(\mathbf{k},\omega)$ at all $k$ and $\omega$; however, the calculations[23] become technically complicated as $k$ increases. In the present work we show that, by using analogs of Ward intensities in orthogonal correlated basis perturbation theories (OCBPT), it is possible to calculate the $S(\mathbf{k},\omega)$ in the scaling limit, and thus extend this low $k$ method to the $k\to\infty$ limit. The OCBPT is reviewed in Sec. II, and the scaling behavior of $S(\mathbf{k},\omega)$ is proved with OCBPT in Sec. III. The $J(y)$ is calculated in Sec. IV approximately by summing all diagrams in which the struck particle emits or absorbs any number of phonons one at a time. This approximation allows intermediate states with any number of phonons, and hence it should be reasonable. It is possible to test its accuracy as discussed in Sec. V. The properties of $J(y)$ calculated with the OCBPT are discussed in Sec. V in a pedagogical fashion, where it is shown that for a weakly interacting system the OCBPT $J(y)$ equals the $J_{\mathrm{IA}}(y)$. Moreover, we find that the analytic structure of the $J(y)$ has singularities found in the $J_{\mathrm{IA}}(y)$ due to the presence of condensate $\delta$ function and the $1/q$ singularities in $n(q)$. The $J(y)$ of liquid $^4$He is calculated in Sec. VI using the experimental $S(q)$. The calculated $J(y)$ is quite similar, though not exactly the same, as the $J_{\mathrm{IA}}(y)$ calculated from theoretical models of $n(q)$. In particular it has a $\delta$ function at $y=0$ of strength comparable with the condensate fraction in $n(q)$. Finally the results of the paper are summarized in Sec. VII. The new techniques developed in this work are fully discussed in the text with the hope that they would be useful in calculating the $S(\mathbf{k},\omega)$ at large but finite $k$ and thus help evolve a unified theory of DSF at all values of $k$ and $\omega$. Nevertheless, to keep the text in sections relatively simple a number of details and proofs are given in the Appendices.

## II. OCB FORMALISM

In the correlated basis (CB) theories of quantum liquids the CB states are defined as[15]

$$|\mathbf{p}_1,\ldots,\mathbf{p}_n)\equiv\frac{G|\mathbf{p}_1,\ldots,\mathbf{p}_n]}{[\mathbf{p}_1,\ldots,\mathbf{p}_n|G^\dagger G|\mathbf{p}_1,\ldots,\mathbf{p}_n]^{1/2}}\ , \quad (2.1)$$

where $|\,]$ are noninteracting states of the ideal gas, and $G$ is the correlation operator which is usually determined by minimizing the ground-state energy

$$E_0=(0|H|0)\equiv\frac{[0|G^\dagger HG|0]}{[0|G^\dagger G|0]}\ . \tag{2.2}$$

If, as is often done in the case of bose liquids,[24] $G|0]$ is taken to be equal to the exact ground state $\Psi_0\equiv|0\rangle$ the Feynman phonon (*FP*) basis is obtained:

$$|\mathbf{p}_1,\ldots\mathbf{p}_n)=\frac{(\rho^\dagger_{\mathbf{p}_1}\cdots\rho^\dagger_{\mathbf{p}_n})|0\rangle}{\langle 0|(\rho_{\mathbf{p}_1}\cdots\rho_{\mathbf{p}_n})(\rho^\dagger_{\mathbf{p}_1}\cdots\rho^\dagger_{\mathbf{p}_n})|0\rangle^{1/2}}\ , \tag{2.3}$$

where

$$(\rho^\dagger_{\mathbf{p}_1}\cdots\rho^\dagger_{\mathbf{p}_n})\equiv\sum_{\substack{i,\cdots,l\\(i\neq\cdots\neq l)}}\frac{1}{\sqrt{N}}\cdots\frac{1}{\sqrt{N}}\times\exp[i(\mathbf{p}_1\cdot\mathbf{r}_i+\cdots+\mathbf{p}_n\cdot\mathbf{r}_l)]\ , \tag{2.4}$$

and $N$ is the number of particles. We will assume the thermodynamic limit $N\to\infty$, $\Omega\to\infty$ at constant density $\rho=N/\Omega$. Note that in this notation $\rho^\dagger_{\mathbf{p}_1}\cdots\rho^\dagger_{\mathbf{p}_n}$ does not equal $(\rho^\dagger_{\mathbf{p}_1}\cdots\rho^\dagger_{\mathbf{p}_n})$ with brackets. The simple product of $\rho^\dagger_{\mathbf{p}}$'s contains terms where particles $i,j,\ldots$ in the sum are the same. Such terms are excluded from the product in the brackets by definition [eq. (2.4)]. CB states are complete and normalized, but not mutually orthogonal. There are continuum many CB states, so that they cannot be orthogonalized using the well-known Schmidt procedure. They can be orthogonalized using the Löwdin transformation,[25] but the resulting states have higher energies than CB states; in particular, the ground-state expectation value of the Hamiltonian is higher. Perturbative corrections move the energies down again, and both of these effects are larger than the net displacement.[15] Hence generally the CB states have been used with a nonorthogonal basis perturbation theory.

Recently, a new orthogonalization procedure free of the problems mentioned above was proposed.[26] A combination of Schmidt and Löwdin transformation is used in such a way that the diagonal matrix elements of the orthonormal-correlated (OCB) and the CB states are equal. First, a partially orthogonal (PO) set of $n$-phonon states is defined using Schmidt procedure:

$$|\mathbf{p}_1,\ldots,\mathbf{p}_n\}\equiv|\mathbf{p}_1,\ldots,\mathbf{p}_n)-\sum_{m<n}\sum_{\mathbf{q}_1,\ldots,\mathbf{q}_m}|\mathbf{q}_1,\ldots,\mathbf{q}_m\rangle\langle\mathbf{q}_1,\ldots,\mathbf{q}_m|\mathbf{p}_1,\ldots,\mathbf{p}_n)\ . \tag{2.5}$$

A PO $n$-phonon state is orthogonal to all PO $(m\neq n)$-phonon states by construction. However, it is not orthogonal to other PO $n$-phonon states. This is achieved in the second step by the Löwdin transformation:

$$|\mathbf{p}_1,\ldots,\mathbf{p}_n\rangle=|\mathbf{p}_1,\ldots,\mathbf{p}_n\}-\frac{1}{2}\sum_{\mathbf{p}'_1,\ldots,\mathbf{p}'_n}|\mathbf{p}'_1,\ldots,\mathbf{p}'_n\}\overline{\{\mathbf{p}'_1,\ldots,\mathbf{p}'_n|\mathbf{p}_1,\ldots,\mathbf{p}_n\}}$$
$$+\frac{3}{8}\sum_{\mathbf{p}'_1,\ldots,\mathbf{p}'_n}\sum_{\mathbf{p}''_1,\ldots,\mathbf{p}''_n}|\mathbf{p}''_1,\ldots,\mathbf{p}''_n\}\overline{\{\mathbf{p}''_1,\ldots,\mathbf{p}''_n|\mathbf{p}'_1,\ldots,\mathbf{p}'_n\}}\,\overline{\{\mathbf{p}'_1,\ldots,\mathbf{p}'_n|\mathbf{p}_1,\ldots,\mathbf{p}_n\}}-\cdots\ , \tag{2.6}$$

where the coefficients $1,-1/2,3/8,\ldots$ are the same as those in the expansion of $(1+x)^{-1/2}$, and a bar on the matrix elements indicates that the diagonal matrix elements are to be omitted. In general we use $|i\rangle,|j\rangle,\ldots$ to denote OCB states. These may also be denoted by listing all momentum labels whenever appropriate.

It is expected that the OCBPT has a better convergence that the nonorthogonal CBPT. Moreover, OCBPT uses the well-known simple perturbation expansions instead of the nonorthogonal perturbation theory. On the other hand, the computation of the matrix elements is more involved due to the complexity of OCB states. The convergence of OCBPT is not expected to depend upon the specific nature of the bare interaction, i.e., if it has a hard core or not. For this reason we use it to study the scaling properties of the response at large $k$ and $\omega$.

It is useful to recall some simple properties of Feynman phonon states. Their normalizations are determined by the static structure function $S(q)$:

$$\langle 0|\rho_{\mathbf{k}}\rho^\dagger_{\mathbf{k}}|0\rangle=S(k)\ , \tag{2.7}$$

$$\langle 0|(\rho_l\rho_{\mathbf{m}}\cdots\rho_{\mathbf{n}})(\rho^\dagger_l\rho^\dagger_{\mathbf{m}}\cdots\rho^\dagger_{\mathbf{n}})|0\rangle=S(l)S(m)\cdots S(n)+\text{terms of order } N^{-1}\ . \tag{2.8}$$

Their energies are obtained from the identity

$$\langle 0|\,A(H-E_0)B\,|0\rangle=\sum_{i=1,N}\frac{1}{2m}\langle 0|(\nabla_i A)\cdot(\nabla_i B)|0\rangle\ , \tag{2.9}$$

where $A$ and $B$ are functions of particle coordinates, like $\rho_l\rho_{\mathbf{m}}\cdots\rho_{\mathbf{n}}$, which commute with the potential. Further, since OCB and CB states have the same diagonal matrix elements of $H$ we obtain

$$\langle\mathbf{k}|H-E_0|\mathbf{k}\rangle=(\mathbf{k}|H-E_0|\mathbf{k})=\frac{\langle 0|\rho_{\mathbf{k}}(H-E_0)\rho^\dagger_{\mathbf{k}}|0\rangle}{\langle 0|\rho_{\mathbf{k}}\rho^\dagger_{\mathbf{k}}|0\rangle}=\frac{k^2}{2mS(k)}\ , \tag{2.10}$$

$$\langle l,\mathbf{m},\ldots,\mathbf{n}|H-E_0|l,\mathbf{m},\ldots,\mathbf{n}\rangle = \frac{l^2}{2mS(l)}+\frac{m^2}{2mS(m)} + \cdots + \frac{n^2}{2mS(n)} + \text{terms of order } N^{-1} . \quad (2.11)$$

The nondiagonal matrix elements are more difficult to calculate. The most important of these are

$$(l,\mathbf{m}|\mathbf{k}) = \frac{1}{\sqrt{N}}\frac{1}{\sqrt{S(k)S(l)S(m)}}\{[S(l)-1]+[S(m)-1]\} \times\delta(\mathbf{k}-l-\mathbf{m})+\text{three-body terms} , \quad (2.12)$$

$$(l,\mathbf{m}|H-E_0|\mathbf{k}) = \frac{1}{\sqrt{N}}\frac{1}{\sqrt{S(k)S(l)S(m)}}\frac{1}{2m} \times\{\mathbf{k}\cdot\mathbf{m}[S(l)-1]+\mathbf{k}\cdot l[S(m)-1]\} \times\delta(\mathbf{k}-l-\mathbf{m})+\text{three-body terms} . \quad (2.13)$$

The above matrix element is the leading term of the OCB matrix element $\langle l,\mathbf{m}|H|\mathbf{k}\rangle$, and can be used to study its properties as shown in Appendix A. It is also shown there that when $k$ is large the three-body terms can be neglected.

The static structure function $S(q)$ of a Bose liquid approaches unity exponentially even when the interatomic interactions are hard, like, for example, the Lenard-Jones (6,12) potential. We do not address here the problem of hard sphere gas whose $[S(q)-1]$ does not go exponentially to zero at large $q$ due to the singularity in the derivative of the pair distribution function $g(r)$ at $r=c$ the hard core radius. In systems like $^4$He liquid whose $[S(q)-1]$ goes to zero exponentially at large $q$, the matrix elements (2.12) and (2.13) are nonzero only for finite values of $l$ and/or $\mathbf{m}$. Hence, when $\mathbf{k}$ is large either $l$ or $\mathbf{m}$ has to be $\sim\mathbf{k}$ so that the other is finite. In other words a hard phonon having a large $\mathbf{k}$ can only emit soft phonons having finte momenta. The main differences between ordinary and OCB perturbation theories are due to this property of Feynman phonons. In ordinary perturbation theory a particle with a large momentum $\mathbf{k}$ can transfer momenta of order $\mathbf{k}$ to another particle when the interparticle interactions have a hard core, whereas a Feynman phonon having a large momentum $\mathbf{k}$ can only transfer a finite momentum even when the interparticle interactions have a hard core. However, the matrix element (2.13) has terms proportional to $\mathbf{k}\cdot l$, and thus becomes very strong in the $k\to\infty$ limit.

## III. SCALING PROPERTY OF DSF

The DSF is given by[15]

$$S(\mathbf{k},\omega)=-\frac{1}{\pi}\mathrm{Im}D(\mathbf{k},\omega) , \quad (3.1)$$

where

$$D(\mathbf{k},\omega)=\langle 0|\rho_{\mathbf{k}}[\omega-H+E_0+i\eta]^{-1}\rho_{\mathbf{k}}^{\dagger}|0\rangle \quad (3.2)$$

$$=S(k)\langle\mathbf{k}|[\omega-H+E_0+i\eta]^{-1}|\mathbf{k}\rangle \quad (3.3)$$

is the density-density response function (DDRF), and $\eta$ is a positive infinitesimal. The Hamiltonian of the system is divided into diagonal and off-diagonal parts with respect to OCB:

$$H=H_0+H' , \quad (3.4)$$

$$\langle i|H_0|j\rangle=\delta_{ij}\langle i|H|i\rangle , \quad (3.5)$$

$$\langle i|H'|j\rangle=(1-\delta_{ij})\langle i|H|j\rangle . \quad (3.6)$$

The resolvent in DDRF can be expanded as

$$D(\mathbf{k},\omega)=S(k)\sum_{n=0}^{\infty}\langle\mathbf{k}|[\omega-H_0+E_0+i\eta]^{-1}(H'[\omega-H_0+E_0+i\eta]^{-1})^n|\mathbf{k}\rangle =S(k)\left[G_0(\mathbf{k})+G_0(\mathbf{k})\left[\sum_i H'_{\mathbf{k}i}G_0(i)H'_{i\mathbf{k}}\right]G_0(\mathbf{k})+\cdots\right] =S(k)G_0(\mathbf{k})+G_0(\mathbf{k})\Sigma(\mathbf{k},\omega)D(\mathbf{k},\omega) , \quad (3.7)$$

where

$$G_0(i)=\langle i|[\omega-H_0+E_0+i\eta]^{-1}|i\rangle \quad (3.8)$$

are energy denominators, and the proper self-energy (PSE) is defined as

$$\Sigma(\mathbf{k},\omega)=\sum_i H'_{\mathbf{k}i}G_0(i)H'_{i\mathbf{k}} + \sum_{i,j}H'_{\mathbf{k}i}G_0(i)H'_{ij}G_0(j)H'_{j\mathbf{k}}+\cdots . \quad (3.9)$$

The above resolvent expansion is well behaved in the sense that every term is finite. This is to be compared with the Gersh-Rodriguez series[19] where every term diverges if the potential has a hard core. The difference comes from the fact that the basis states used to derive Gersh-Rodriquez series (plane waves for the struck atom and exact eigenstates for the remaining $N-1$ atoms) do not include the strong short-range correlations between the struck atom and the rest of the atoms, whereas OCB states do.

When $k$ is large, $S(k)=1$, and from Eq. (2.10) we obtain

$$G_0(k)=\left[\omega-\frac{k^2}{2m}+i\eta\right]^{-1}=\frac{m}{k}(y+i\eta)^{-1} , \quad (3.10)$$

$$D(\mathbf{k},\omega)=\left[\omega-\frac{k^2}{2m}-\Sigma(\mathbf{k},\omega)+i\eta\right]^{-1} . \tag{3.11}$$

Moreover, as discussed in Sec. II, and proved in Appendix A, only the states $|i\rangle$ that have one hard phonon with momentum of order $k$ and one or more soft phonons with finite momenta contribute to $\Sigma(\mathbf{k},\omega)$. These states are represented as

$$|i\rangle=|\mathbf{k}-\mathbf{p}_1-\cdots-\mathbf{p}_{n-1},\mathbf{p}_1,\ldots,\mathbf{p}_{n-1}\rangle , \tag{3.12}$$

where $|\mathbf{p}_i|$ are finite, i.e., of order $k^0$, and

$$G_0(i)=\left[\omega-\frac{1}{2m}(\mathbf{k}-\mathbf{p}_1-\cdots-\mathbf{p}_{n-1})^2+O(k^0)+i\eta\right]^{-1}$$

$$=\frac{m}{k}[g_0(i)+O(k^{-1})+i\eta]^{-1} , \tag{3.13}$$

$$g_0(i)=y-\hat{\mathbf{k}}\cdot(\mathbf{p}_1+\cdots+\mathbf{p}_{n-1}) . \tag{3.14}$$

In Appendix A it is also proved that the off-diagonal matrix elements $H'_{ij}$ between states having one hard phonon are proportional to $k/m$, i.e.,

$$H'_{ij}=\frac{k}{m}[h'_{ij}+O(k^{-1})] , \tag{3.15}$$

where $h'_{ij}$ is independent of $k$. From Eqs. (3.9), (3.13), and (3.15) it follows that

$$\frac{m}{k}\Sigma(\mathbf{k},\omega)=\Sigma_S(y)+O(k^{-1}) , \tag{3.16}$$

$$\Sigma_S(y)=\sum_i h'_{ki}g_0(i)h'_{ik}+\sum_{i\neq j}h'_{ki}g_0(i)h'_{ij}g_0(j)h'_{jk}+\cdots . \tag{3.17}$$

Consequently

$$\frac{k}{m}D(\mathbf{k},\omega)=D_S(y)+O(k^{-1}) , \tag{3.18}$$

$$D_S(y)=[y-\Sigma_S(y)+i\eta]^{-1} , \tag{3.19}$$

so that $(k/m)S(\mathbf{k},\omega)$ [Eq. (3.1)] is a function of $y$ alone in the limit $k\to\infty$, and $y$ scaling is found to be an exact result. We also obtain the useful relation

$$1-yD_S(y)=\frac{-\Sigma_S(y)}{y-\Sigma_S(y)+i\eta} \tag{3.20}$$

from Eq. (3.19).

## IV. CALCULATION OF THE SCALING FUNCTION

It can be shown that spectator phonons do not contribute to the matrix elements of OCB,[26] i.e.,

$$\langle\mathbf{p}_1,\ldots,\mathbf{p}_n,\mathbf{q}_1,\ldots,\mathbf{q}_m|H|\mathbf{p}'_1,\ldots,\mathbf{p}'_{n'},\mathbf{q}_1,\ldots,\mathbf{q}_m\rangle$$

$$=\langle\mathbf{p}_1,\ldots,\mathbf{p}_n|H|\mathbf{p}'_1,\ldots,\mathbf{p}'_{n'}\rangle \tag{4.1}$$

when the number of phonons $(n+m)$ and $(n'+m)$ is finite. Because of this property it is possible to consider the diagrammatic expansion of $\Sigma_S(y)$ shown in Fig. 1, where the thick line represents the hard phonon and thin lines represent soft phonons. An exact calculation of

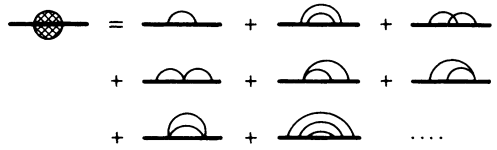

FIG. 1. The expansion of the self-energy $\Sigma_S(y)$ [Eq. (3.17)]. The thick line represents the hard phonon while the thin lines represent the soft phonons.

$\Sigma_S(y)$ is difficult because of the large number of different types of vertices, representing the matrix elements $h'_{ij}$, in this expansion. However, all the diagrams based on the vertex at which the hard phonon emits or absorbs a soft phonon, as illustrated in Fig. 2(a), can be summed by the standard field-theoretical methods.

In Appendix B it is shown that this basic one- to two-phonon vertex is given by

$$\frac{m}{k}\langle\mathbf{k}|H|\mathbf{k}-l,l\rangle\equiv\Gamma_0(l)+O(k^{-1})$$

$$=-\frac{1}{\sqrt{N}}\frac{\hat{\mathbf{k}}\cdot\hat{\mathbf{l}}}{2}\sqrt{f(l)}+O(k^{-1}) . \tag{4.2}$$

The function $f(l)$ is determined entirely by the static

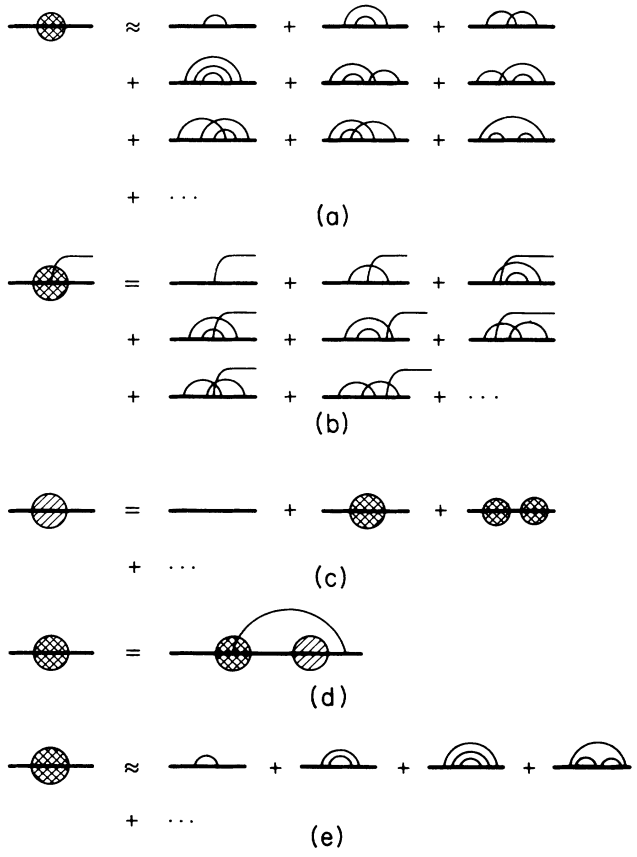


FIG. 2. Diagrammatic representation of terms that include only the one- to two-phonon vertex. (a) The proper self-energy $\Sigma_S(y)$. (b) The dressed vertex $\Gamma(l,y)$. (c) The dressed hard phonon propagator $g(y)$. (d) The Dyson equation. (e) Nonintersecting diagrams of $\Sigma'_S(y)$.

structure function $S(q)$, and is also calculated in Appendix B. It contains a leading term

$$f_0(l)=l^2\frac{[S(l)-1]^2}{S(l)} \tag{4.3}$$

and small corrections from the Löwdin orthogonalization of the two-phonon states. The $f(l)$ is finite and linear in $l$ at small $l$ where $S(l)$ is linear in $l$. We recall that $S(q)$ is the only input in our calculation of the scaling function, as opposed to other works where the ground-state momentum distribution $n(q)$ is used.

Since we closely follow the calculation of electron self-energy in QED, it is natural to use the same terminology whenever possible. Thus the dressed vertex $\Gamma(l,y)$ is defined as

$$\Gamma(l,y)=\Gamma_0(l)[1+\Lambda(l,y)] \tag{4.4}$$

and it represents the sum of diagrams in Fig. 2(b); $\Lambda(l,y)$ is the vertex correction. The dressed hard phonon propagator $g(y)$ is shown in Fig. 2(c), and the Dyson equation for the proper self-energy is shown in Fig. 2(d). Analytically it is written as

$$\Sigma_S(y)=\sum_l \Gamma(l,y)g(y+\hat{\mathbf{k}}\cdot\mathbf{l})\Gamma_0(l)$$
$$=\int\frac{d^3l}{(2\pi)^3\rho}\frac{(\hat{\mathbf{k}}\cdot\hat{\mathbf{l}})^2 f(l)[1+\Lambda(l,y)]}{4[y+\hat{\mathbf{k}}\cdot\mathbf{l}-\Sigma_S(y+\hat{\mathbf{k}}\cdot\mathbf{l})+i\eta]}\ . \tag{4.5}$$

If we put $\Lambda(l,y)\equiv 0$ in Eq. (4.5), we obtain the integral equation for the sum of all diagrams without intersecting soft phonon lines as is illustrated in Fig. 2(e):

$$\Sigma'_S(y)=\int\frac{d^3l}{(2\pi)^3\rho}\frac{(\hat{\mathbf{k}}\cdot\hat{\mathbf{l}})^2 f(l)}{4[y+\hat{\mathbf{k}}\cdot\mathbf{l}-\Sigma'_S(y+\hat{\mathbf{k}}\cdot\mathbf{l})+i\eta]}\ . \tag{4.6}$$

This integral equation for $\Sigma'_S(y)$ can be easily solved numerically by iteration.

To calculate $\Sigma_S(y)$ including the vertex correction we need another equation relating $\Sigma_S(y)$ to $\Lambda(l,y)$. As mentioned above, the number of hard phonons is conserved in this theory. This conservation is analogous to the charge conservation in QED, and it is not surprising that the identity

$$\hat{\mathbf{k}}\cdot\mathbf{l}\,\Lambda(l,y)=\Sigma_S(y)-\Sigma_S(y+\hat{\mathbf{k}}\cdot\mathbf{l}) \tag{4.7}$$

analogous to the Ward identity of QED holds. The proof of this identity is given in Appendix C. Equation (4.7) is expressed as

$$\hat{\mathbf{k}}\cdot\mathbf{l}[1+\Lambda(l,y)]=[y+\hat{\mathbf{k}}\cdot\mathbf{l}-\Sigma_S(y+\hat{\mathbf{k}}\cdot\mathbf{l})]-[y-\Sigma_S(y)] \tag{4.8}$$

and substituted into Eq. (4.5) to obtain

$$\Sigma_S(y)=\int\frac{d^3l}{(2\pi)^3\rho}\frac{\hat{\mathbf{k}}\cdot\hat{\mathbf{l}}f(l)\{[y+\hat{\mathbf{k}}\cdot\mathbf{l}-\Sigma_S(y+\hat{\mathbf{k}}\cdot\mathbf{l})]-[y-\Sigma_S(y)]\}}{4l[y+\hat{\mathbf{k}}\cdot\mathbf{l}-\Sigma_S(y+\hat{\mathbf{k}}\cdot\mathbf{l})+i\eta]}$$
$$=-[y-\Sigma_S(y)]\int\frac{d^3l}{(2\pi)^3\rho}\frac{\hat{\mathbf{k}}\cdot\hat{\mathbf{l}}f(l)}{4l[y+\hat{\mathbf{k}}\cdot\mathbf{l}-\Sigma_S(y+\hat{\mathbf{k}}\cdot\mathbf{l})+i\eta]}\ . \tag{4.9}$$

Substituting this $\Sigma_S(y)$ into the RHS of Eq. (3.20), we obtain

$$1-yD_S(y)=\int\frac{d^3l}{(2\pi)^3\rho}\frac{\hat{\mathbf{k}}\cdot\hat{\mathbf{l}}f(l)}{4l[y+\hat{\mathbf{k}}\cdot\mathbf{l}-\Sigma_S(y+\hat{\mathbf{k}}\cdot\mathbf{l})+i\eta]}$$
$$=\int\frac{d^3l}{(2\pi)^3\rho}\hat{\mathbf{k}}\cdot\hat{\mathbf{l}}\frac{f(l)}{4l}D_S(y+\hat{\mathbf{k}}\cdot\mathbf{l})$$
$$=\frac{1}{16\pi^2\rho}\int_{-\infty}^{\infty}dl_z D_S(y+l_z)l_z F(l_z)\ , \tag{4.10}$$

where

$$F(x)\equiv\int_0^\infty d\rho\,\rho\frac{f(\sqrt{\rho^2+x^2})}{\rho^2+x^2}=\int_{|x|}^\infty dt\frac{f(t)}{t}\ . \tag{4.11}$$

At small $t$ the function $f(t)$ is linear in $t$ so that $F(x)$ is finite and continuous at $x=0$. Moreover, it is real and decreasing since $f(t)$ is real and positive. Since $\mathrm{Im}D_S(y)=-\pi J(y)$ it follows that

$$yJ(y)=a\int_{-\infty}^{\infty}dz(y-z)F(y-z)J(z)\ , \tag{4.12}$$

where $a=1/16\pi^2\rho$.

Equation (4.12) is of a convolution type, and can be solved by Fourier transform. Functions $J(y)$ and $F(x)$ are absolutely integrable:

$$\int_{-\infty}^{\infty}dy\,|J(y)|=\int_{-\infty}^{\infty}dy\,J(y)=1\ , \tag{4.13}$$

$$\int_{-\infty}^{\infty}dx\,|F(x)|=\int_{-\infty}^{\infty}dx\int_0^\infty d\rho\,\rho\frac{f(\sqrt{\rho^2+x^2})}{\rho^2+x^2}$$
$$=\frac{1}{2\pi}\int d^3r\frac{f(r)}{r^2}=2\int_0^\infty dx\,f(x)<\infty\ , \tag{4.14}$$

so that their Fourier transforms are defined. Using the identity $i\tilde{f}'(s)=\int_{-\infty}^{\infty}dy\,e^{-iys}yf(y)$ the integral equation (4.12) can be reduced to the differential equation

$$\tilde{J}'(s)=a\tilde{F}'(s)\tilde{J}(s)\ , \tag{4.15}$$

which has the solution

$$\tilde{J}(s)=Ce^{a\tilde{F}(s)}\ . \tag{4.16}$$

In the limit $s\to\infty$ $\tilde{F}(s)\to 0$, and hence $\tilde{J}(s)\to C$. Thus, inverting Fourier transform gives

$$J(y)=C\delta(y)+C\int_{-\infty}^{\infty}\frac{ds}{2\pi}e^{iys}\times\left[\exp\left[a\int_{-\infty}^{\infty}dx\,e^{-ixs}F(x)\right]-1\right]. \tag{4.17}$$

The constant $C$ can be found from the normalization condition

$$1=\int_{-\infty}^{\infty}dy\,J(y)=C\left[1+\exp\left[a\int_{-\infty}^{\infty}dx\,F(x)\right]-1\right],$$
$$C=\exp\left[-2a\int_0^{\infty}dx\,F(x)\right]=\exp\left[-2a\int_0^{\infty}dl\,f(l)\right]. \tag{4.18}$$

Formulas (4.17) and (4.18) are the main result of the present paper.

## V. DISCUSSION

We begin the analysis of the scaling function $J(y)$ [Eq. (4.17)] by evaluating it in the limit $y\to 0$. In this limit the function $F(y)$ [Eq. (4.11)] can be expanded as follows:

$$F(y\to 0)=F(0)-|y|\lim_{l\to 0}\frac{f(l)}{l}+O(y^2). \tag{5.1}$$

In Appendix B it is shown that the slope of the $f(l)$ at the origin is the same as that of $f_0(l)$ [Eq. (4.3)] so that

$$\lim_{l\to 0}\frac{f(l)}{l}=\lim_{l\to 0}\frac{f_0(l)}{l}=\lim_{l\to 0}\frac{l}{S(l)}=2mc, \tag{5.2}$$

where $c$ is the sound velocity in the liquid, and we obtain

$$F(y\to 0)=F(0)-2mc|y|+O(y^2). \tag{5.3}$$

The function $F(y)$ has a cusp at $y=0$, and we will now show that as a consequence the scaling function $J(y)$ has a cusp at the origin in addition to the $\delta$ function. In the theory of Fourier transforms[27] it is proved that for sufficiently smooth functions $\Phi(x)$:

$$\int_0^{\infty}dx\cos(sx)\Phi(x)=-\frac{\Phi'(0)}{s^2}+\frac{\Phi'''(0)}{s^4}-\frac{\Phi^{(V)}(0)}{s^6}+\cdots\quad s\to\infty. \tag{5.4}$$

Thus, the Fourier transform of the function $F(x)$ is

$$\tilde{F}(s\to\infty)=2\int_0^{\infty}dx\cos(sx)F(x)=\frac{4mc}{s^2}+O\left[\frac{1}{s^4}\right], \tag{5.5}$$

so that the integrand of Eq. (4.17) becomes

$$e^{a\tilde{F}(s)}-1=\frac{4amc}{s^2}+O\left[\frac{1}{s^4}\right]=\frac{1}{4\pi^2\rho}\frac{mc}{s^2}+O\left[\frac{1}{s^4}\right]\quad s\to\infty. \tag{5.6}$$

From Eqs. (4.17), (5.4), and (5.6) it follows that

$$J(y\to 0)=C\delta(y)+\frac{1}{4\pi^2\rho}[A-B|y|], \tag{5.7}$$

where the constant $C$ is given by Eq. (4.18), and the constants $A$ and $B$ are given by

$$A=4\pi\rho C\int_0^{\infty}ds\left[\exp\left[\frac{1}{8\pi^2\rho}\int_0^{\infty}dx\cos(sx)F(x)\right]-1\right], \tag{5.8}$$

$$B=C\frac{mc}{2}. \tag{5.9}$$

The scaling function in IA [Eq. (1.2)] exhibits the same small $y$ behavior with the coefficients

$$C_{\rm IA}=n_c,\quad A_{\rm IA}=\int_0^{\infty}dq\,qn(q),\quad B_{\rm IA}=\lim_{q\to 0}qn(q)=n_c\frac{mc}{2}. \tag{5.10}$$

In particular the ratio $B/C$ is identical in both our theory and IA.

Next, we want to discuss the origin of the $\delta$-function peak at $y=0$. In general, the presence of the $\delta$ function in DSF means that the probe couples to a long-lived state with a given energy and momentum. The inverse lifetime of this excitation is given by the imaginary part of the self-energy: $\tau^{-1}\sim\mathrm{Im}\,\Sigma(\mathbf{k},\omega)$, and it is expected to be proportional to $k$ on the basis of the semiclassical value $\tau\sim\rho v\sigma$, where $\rho$ is the density, $v\equiv k/m$ the velocity, and $\sigma$ the average two-body scattering cross section. The $\mathrm{Im}\,\Sigma(\mathbf{k},\omega)$ depends upon $y$, and it is order $k$ when $y\neq 0$. However, in the present calculation the $\mathrm{Im}\,\Sigma(\mathbf{k},\omega)$ at $y=0$ does not have a term of order $k$, and hence the $\delta$ function at $y=0$ in the $J(y)$.

The origin of the $y$ dependence of the lifetime can be easily seen in the contribution of the second-order diagram, i.e., the first diagram of Fig. 2(a). In second order, an off-shell FP with momentum $\mathbf{k}$ and energy $\omega=k^2/2m+ky/m$ can decay into two FP of momenta $\mathbf{k}-\mathbf{l}$ and $\mathbf{l}$, thus acquiring a lifetime given by

$$\frac{1}{\tau}=2\pi\int\frac{d^3l}{(2\pi)^3\rho}|\langle\mathbf{k}-\mathbf{l},\mathbf{l}|H|\mathbf{k}\rangle|^2\times\delta(\omega-(\mathbf{k}-\mathbf{l})^2/2m-l^2/2mS(l)). \tag{5.11}$$

Using Eqs. (4.2) and (5.11) we obtain

$$\frac{1}{\tau}=\frac{1}{4(2\pi)^2\rho}\frac{k}{m}\int d^3l(\hat{\mathbf{k}}\cdot\hat{\mathbf{l}})^2f(l)\delta(y+\hat{\mathbf{k}}\cdot\mathbf{l}+O(k^{-1})). \tag{5.12}$$

When $y\neq 0$ we get $\tau\sim k^{-1}$ as expected from semiclassical arguments, but when $y=0$ (on-shell FP) the situation is completely different. In that case the energy-conserving $\delta$ function forces the cosine $\hat{\mathbf{k}}\cdot\hat{\mathbf{l}}$ to be of the order $k^{-1}$ which makes the integrand of Eq. (5.12) small, and we find that on-shell FP has a long lifetime $\tau\sim k$ in this order.

The $\Sigma_S(y)$ of Eq. (4.9) has the properties

$$\mathrm{Re}\,\Sigma_S(-y)=-\mathrm{Re}\,\Sigma_S(y), \tag{5.13}$$

$$\mathrm{Im}\,\Sigma_S(-y)=\mathrm{Im}\,\Sigma_S(y), \tag{5.14}$$

$$\Sigma_S(0)=0. \tag{5.15}$$

The solution of the simpler integral equation (4.6), obtained by summing diagrams of Fig. 2(e), also satisfies the symmetry properties (5.13) and (5.14); however,

$$\mathrm{Im}\,\Sigma_S'(0)\neq 0\ . \tag{5.16}$$

Hence the scaling function $J(y)$ obtained from the $\Sigma_S'(y)$ does not have a $\delta$ function at $y=0$. The approximation $\Sigma_S'(y)$ is bad since there is an exact cancellation between the summed and the omitted diagrams at $y=0$. This cancellation occurs order by order in loopwise expansion of $\Sigma_S(y)$. We will demonstrate it on a two-loop level, i.e., we will show that the sum of the second and the third diagrams on Fig. 2(a) vanishes at $y=0$. We denote this sum $\Sigma_S^{(2)}(y)$ and obtain

$$\begin{aligned}\Sigma_S^{(2)}(0)&=\int\frac{d^3l}{(2\pi)^3\rho}\frac{d^3m}{(2\pi)^3\rho}\frac{(\hat{\mathbf{k}}\cdot\hat{\mathbf{l}})^2(\mathbf{k}\cdot\hat{\mathbf{m}})^2 f(l)f(m)}{16(\hat{\mathbf{k}}\cdot\mathbf{l}+i\eta)[\hat{\mathbf{k}}\cdot(\mathbf{l}+\mathbf{m})+i\eta]}\left[\frac{1}{\hat{\mathbf{k}}\cdot\mathbf{l}+i\eta}+\frac{1}{\hat{\mathbf{k}}\cdot\mathbf{m}+i\eta}\right]\\&=\int\frac{d^3l}{(2\pi)^3\rho}\frac{d^3m}{(2\pi)^3\rho}\frac{\hat{\mathbf{k}}\cdot\mathbf{m}f(l)f(m)}{16l^2m^2[\hat{\mathbf{k}}\cdot(\mathbf{l}+\mathbf{m})+i\eta]}(\hat{\mathbf{k}}\cdot\mathbf{l}+\hat{\mathbf{k}}\cdot\mathbf{m})\\&=\int\frac{d^3l}{(2\pi)^3\rho}\frac{d^3m}{(2\pi)^3\rho}\frac{\hat{\mathbf{k}}\cdot\mathbf{m}f(l)f(m)}{16l^2m^2}=0\ .\end{aligned} \tag{5.17}$$

In the present calculation it was possible to sum all the diagrams containing one- to two-phonon vertex [Fig. 2(a)], and thus preserve this cancellation. If, for some reason, the $J(y)$ has to be approximated by a subset of diagrams, then it appears that the correct way to do it is to sum the diagrams order by order in the interaction rather than to sum infinite subsets of diagrams like $\Sigma_S'(y)$.

In our calculation of the scaling function $J(y)$, we have taken into account only the diagrams containing one- to two-phonon vertex. We can estimate the validity of this approximation by calculating the known sum rules:[15]

$$\int_{-\infty}^{\infty}dy\,J(y)=1\ , \tag{5.18}$$

$$\int_{-\infty}^{\infty}dy\,yJ(y)=0\ , \tag{5.19}$$

$$\int_{-\infty}^{\infty}dy\,y^2J(y)=\frac{2m}{3}E_k\ , \tag{5.20}$$

where $E_k$ is the ground-state kinetic energy per particle. The first two sum rules are satisfied by the construction of $J(y)$ [Eq. (4.17)], and for the third we obtain

$$\int_{-\infty}^{\infty}dy\,y^2J(y)=\frac{1}{24\pi^2\rho}\int_0^{\infty}dl\,l^2f(l)\ . \tag{5.21}$$

However, since Eq. (4.17) is not exact, the right-hand side of Eq. (5.21) may be different from $2mE_k/3$, and the difference is a measure of the importance of the neglected one- to many-phonon diagrams.

Finally, we want to show that in the uniform limit $[|g(r)-1|\ll 1]$ the scaling function $J(y)$ [Eqs. (4.17) and (4.18)] equals to the $J_{\mathrm{IA}}(y)$. The uniform limit[15] is the situation where the radial distribution function is very near to unity:

$$g(r)=1-\alpha G(s),\quad s\equiv(\alpha\rho)^{1/3}r,\quad G(0)=1\ , \tag{5.22}$$

where $\alpha$ is a small parameter. Physically, it corresponds to the dense ($\rho\to\infty$) systems with regular interaction, although it can be realized even in dilute ($\rho\to 0$) systems provided that the potential is sufficiently weak. The static structure function is given by

$$S(q)=1-F(p),\quad p\equiv(\alpha\rho)^{-1/3}q,\quad F(0)=1\ . \tag{5.23}$$

Since $S(q)$ depends only on $p$, each integration over momenta gives an additional power of $\alpha$. Thus, to the lowest order in $\alpha$ the Löwdin corrections [Eq. (B8)] vanish and the function $f(l)$ becomes

$$f_U(l)=\frac{l^2[S(l)-1]^2}{S(l)}=4l^2n(l)\ . \tag{5.24}$$

The above relation between $S(l)$ and $n(l)$ is derived in Ref. 15. Using it the scaling function in the uniform limit becomes

$$\begin{aligned}J_U(y)&=C\delta(y)+\frac{1}{16\pi^2\rho}\int_{|y|}^{\infty}dl\frac{f_U(l)}{l}\\&=C\delta(y)+\frac{1}{4\pi^2\rho}\int_{|y|}^{\infty}dq\,qn(q)\ ,\end{aligned} \tag{5.25}$$

and

$$C=1-\frac{1}{8\pi^2\rho}\int_0^{\infty}dl\,f_U(l)=1-\int\frac{d^3q}{(2\pi)^3\rho}n(q) \tag{5.26}$$

is the fraction of particles in the condensate, as in $J_{\mathrm{IA}}(y)$.

## VI. NUMERICAL RESULTS

In this section we will apply the theory developed in Sec. IV to the liquid $^4$He at zero temperature. First, we compute the vertex function $f(l)$ given by Eq. (B8). As was already mentioned, the only input needed in this computation is the static structure function $S(q)$. Using the experimental $S(q)$ from Ref. 28 we obtain the function $f(l)$ that is shown in Fig. 3 together with its leading part $f_0(l)$ [Eq. (4.3)]. It can be seen that the Löwdin correction [i.e., the difference between $f(l)$ and $f_0(l)$] is small, but it is nevertheless significant since the scaling function $J(y)$ [Eq. (4.17)] and the strength of the $\delta$-function peak [Eq. (4.18)] depend exponentially on $f(l)$.

Using this $f(l)$ in Eqs. (4.17) and (4.18) we obtain $C=0.15$, and the $J(y)$ that is shown in Fig. 4. For comparison, $J_{\mathrm{IA}}(y)$ generated from the variational $n(q)$ (Ref. 29) that has the condensate fraction $n_c=0.092$ is also shown. In order to test the sensitivity of the calculated $J(y)$ to changes in the input, we have computed it using

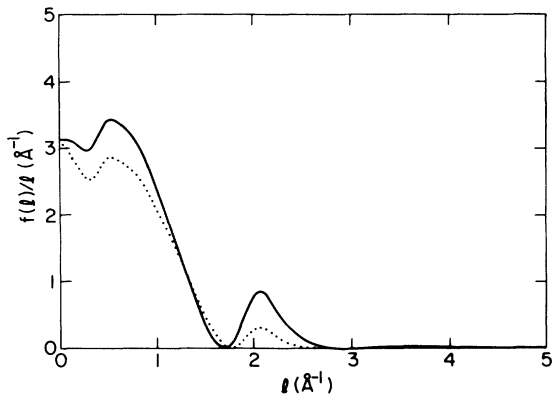


FIG. 3. The function $f(l)/l$ [Eqs. (4.2) and (B8)] of liquid $^4$He at equilibrium density and zero temperature calculated from $S(q)$ of Ref. 28 with (solid line) and without (dotted line) Löwdin corrections.

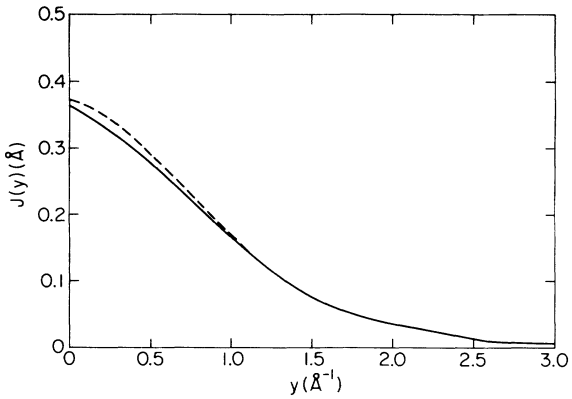


FIG. 4. The scaling functions of liquid $^4$He at equilibrium density and zero temperature. Solid line: Eq. (4.17) using $f(l)$ of Fig. 4; dotted line: IA generated from $n(q)$ of Ref. 29. The $\delta$-function peaks at $y=0$ with respective strengths of 0.15 and 0.092 are implied.

the Monte Carlo $S(q)$ from Ref. 30, and obtained essentially the same result. In particular, in this case $C=0.14$, which is to be compared with $n_c=0.11$ in the Monte Carlo calculation of Ref. 30.

Finally, using the value $E_k=14.8$ K from Ref. 23 and $f(l)$ from Fig. 3, we find that

$$\frac{1}{E_k}\frac{1}{16\pi^2\rho m}\int_0^\infty dl\, l^2 f(l)=0.97\ . \tag{6.1}$$

As was argued in Sec. V, the closeness of this value to 1 suggests that diagrams involving one- to many-phonon vertices have contributions much smaller than those of diagrams containing one- to two-phonon vertex only. However, the numerical value $1-0.97=0.03$ of the error has to be taken only as an estimate since the experimental $S(q)$ and theoretical $E_k$ are used to obtain it.

## VII. CONCLUSIONS

We have presented the calculation of the $S(\mathbf{k},\omega)$ of a bose liquid at $T=0$ in the asymptotic limit $k,\omega\to\infty$, at $y\equiv(m/k)(\omega-k^2/2m)=$const, using OCB formalism. The orthogonalized Feynman phonon states [Eqs. (2.3)–(2.6)] are used to construct the OC basis. It is found that $y$ scaling is exact in the $k\to\infty$ limit, i.e., $(m/k)S(\mathbf{k},\omega)$ is a function of $y$ alone. It is also found that the dominant physical process is emission and absorption of the soft phonons (i.e., phonons whose momenta are $\ll k$) by the hard phonon that is generated by the recoiling atom.

In order to obtain the scaling function $J(y)$ an approximation that amounts to allowing soft phonons to be emitted or absorbed only one at the time is introduced (see Fig. 2). The resulting theory is solved using standard field-theoretical methods without further approximations, and the closed expression for $J(y)$ is obtained [see Eqs. (4.17), (4.18), (4.11), and (B8)–(B10)]. The only input needed is the static structure function $S(q)$ of the system.

It is found that $J(y)$ has a $\delta$-function peak at $y=0$, whose strength is connected with the slope $dJ(y)/dy|_{y=0}$ in the same fashion as in the IA [Eq. (5.9)]. In the case of the liquid $^4$He this strength is equal to 0.15, which is to be compared with the corresponding value of $\sim 0.1$ in the IA that is obtained from the theoretical calculations of the momentum distribution.[29,30] The plot of the calculated $J(y)$ vs $J_{\rm IA}(y)$ for $y\neq 0$ is given in Fig. 4.

Finally, the validity of the approximation made in neglecting processes that involve simultaneous emissions and/or absorptions of multiple phonons is tested in two ways. First, the kinetic energy sum rule for $J(y)$ is evaluated [Eq. (5.21)]. Its numerical closeness to the theoretical value suggests that the neglected processes are not important. Second, it is verified that in the exactly solvable uniform limit $[g(r)-1\ll 1]$ $J(y)$ reduces to the known expression[15] as it should.

## ACKNOWLEDGMENTS

This work was supported in part by the U.S. Department of Energy, Division of Material Sciences Grant No. DE-AC02-76ER01198, and the National Science Foundation Grant No. PHY-89-21025.

## APPENDIX A: PROPERTIES OF OCB MATRIX ELEMENTS

The CB matrix elements of the unit operator and the Hamiltonian are given by

$$(\mathbf{p}_1\cdots\mathbf{p}_n|\mathbf{q}_1\cdots\mathbf{q}_m)=\frac{\langle 0|(\rho_{\mathbf{p}_1}\cdots\rho_{\mathbf{p}_n})(\rho^\dagger_{\mathbf{q}_1}\cdots\rho^\dagger_{\mathbf{q}_m})|0\rangle}{[S(p_1)\cdots S(p_n)S(q_1)\cdots S(q_m)]^{1/2}}\ , \tag{A1}$$

$$(\mathbf{p}_1\cdots\mathbf{p}_n|(H-E_0)|\mathbf{q}_1\cdots\mathbf{q}_m)=\frac{1}{2m}\sum_i\frac{\langle 0|\nabla_i(\rho_{\mathbf{p}_1}\cdots\rho_{\mathbf{p}_n})\cdot\nabla_i(\rho^\dagger_{\mathbf{q}_1}\cdots\rho^\dagger_{\mathbf{q}_m})|0\rangle}{[S(p_1)\cdots S(p_n)S(q_1)\cdots S(q_m)]^{1/2}}\ . \tag{A2}$$

We note that

$$\begin{aligned}&\langle 0|\nabla_i(\rho_{\mathbf{p}_1}\cdots\rho_{\mathbf{p}_n})\cdot\nabla_i(\rho^\dagger_{\mathbf{q}_1}\cdots\rho^\dagger_{\mathbf{q}_m})|0\rangle\\&\quad=\frac{1}{N^{(n+m)/2}}\sum_{\substack{j=1,n\\k=1,m}}\mathbf{p}_j\cdot\mathbf{q}_k\sum_{\substack{i_1\neq\cdots i\cdots\neq i_n\\ i'_1\neq\cdots i\cdots\neq i'_m}}\langle 0|\exp[-i(\mathbf{p}_1\cdot\mathbf{r}_{i_1}+\cdots\mathbf{p}_j\cdot\mathbf{r}_i\cdots+\mathbf{p}_n\cdot\mathbf{r}_{i_n}-\mathbf{q}_1\cdot\mathbf{r}_{i'_1}\\&\qquad\qquad-\cdots\mathbf{q}_k\cdot\mathbf{r}_i\cdots-\mathbf{q}_m\cdot\mathbf{r}_{i'_m})]|0\rangle\ ,\end{aligned} \tag{A3}$$

where in the last sum we are not summing over $i$. These matrix elements vanish if the states $|\mathbf{p}_1\cdots\mathbf{p}_n\rangle$ and $|\mathbf{q}_1\cdots\mathbf{q}_m\rangle$ contain an unequal number of hard phonons. Such matrix elements necessarily contain expectation values of $e^{i\mathbf{k}\cdot\mathbf{r}_{ij}}$ proportional to $S(k)-1$ which vanish at large $k$. The matrix elements do not vanish if the states have an equal number of hard phonons. For example, if $\mathbf{p}_1$ and $\mathbf{q}_1\sim\mathbf{k}$, then terms having particles $i_1=i'_1$ will contribute to (A3). Since the initial state $|\mathbf{k}\rangle$ has one hard phonon, all the states that contribute to $\Sigma(\mathbf{k},\omega)$ [Eq. (3.9)] also must have one hard phonon. We denote them by $|\mathbf{P},\mathbf{p}_1\cdots\mathbf{p}_n\rangle$, where

$$\mathbf{P}=\mathbf{k}-\mathbf{p}_1-\cdots-\mathbf{p}_n\ , \tag{A4}$$

and all lower case $\mathbf{p}_i$ are of order "1", i.e., of order $k^0$. In this case only the following terms contribute to overlap:

$$\begin{aligned}(\mathbf{P},\mathbf{p}_1\cdots\mathbf{p}_n|\mathbf{Q},\mathbf{q}_1\cdots\mathbf{q}_m)&=\frac{1}{N^{(n+m+2)/2}}\\&\times\sum_{\substack{i\neq i_1\neq\cdots\neq i_n\\ i\neq i'_1\neq\cdots\neq i'_m}}\frac{\langle 0|\exp\{-i[(\mathbf{P}-\mathbf{Q})\cdot\mathbf{r}_i+\mathbf{p}_1\cdot\mathbf{r}_{i_1}+\cdots+\mathbf{p}_n\cdot\mathbf{r}_{i_n}-\mathbf{q}_1\cdot\mathbf{r}_{i'_1}-\cdots-\mathbf{q}_m\cdot\mathbf{r}_{i'_m}]\}|0\rangle}{[S(p_1)\cdots S(p_n)S(q_1)\cdots S(q_m)]^{1/2}}\ .\end{aligned} \tag{A5}$$

For this reason only two-body terms contribute to the matrix elements (2.12) and (2.13). We need to consider only the contribution of terms having $\mathbf{P}\cdot\mathbf{Q}$ in Eq. (A3) to the matrix elements of $H-E_0$. These terms give contributions of order $k^2$ and $k$. The terms having $\mathbf{P}\cdot\mathbf{q}_l$ or $\mathbf{p}_l\cdot\mathbf{Q}$ contain expectation values of $e^{i\mathbf{k}\cdot\mathbf{r}_{ii'_l}}$ or $e^{i\mathbf{k}\cdot\mathbf{r}_{i_li}}$, and they vanish in the limit $k\to\infty$, and those having $\mathbf{p}_l\cdot\mathbf{q}_{l'}$ give contributions of order 1 which can be neglected. It then follows that

$$\begin{aligned}(\mathbf{P},\mathbf{p}_1,\ldots,\mathbf{p}_n|(H-E_0)|\mathbf{Q},\mathbf{q}_1,\ldots,\mathbf{q}_m)&=\frac{1}{2m}\left[k^2-\mathbf{k}\cdot\left[\sum_{i=1}^n\mathbf{p}_i+\sum_{j=1}^m\mathbf{q}_j\right]\right]\\&\times(\mathbf{P},\mathbf{p}_1,\ldots,\mathbf{p}_n|\mathbf{Q},\mathbf{q}_1,\ldots,\mathbf{q}_m)+\text{terms of order } k^0\ .\end{aligned} \tag{A6}$$

The diagonal matrix elements of orthogonal correlated (OC) states $|\mathbf{P},\mathbf{p}_1,\ldots,\mathbf{p}_n\rangle$ are the same as those between CB states $|\mathbf{P},\mathbf{p}_1,\ldots,\mathbf{p}_n\rangle$ by construction. However, the nondiagonal elements are different. We can generally write

$$|\mathbf{P},\mathbf{p}_1,\ldots,\mathbf{p}_n\rangle=\sum_{m\le n}\sum_{\mathbf{q}_1,\ldots,\mathbf{q}_m}\alpha(\mathbf{p}_1,\ldots,\mathbf{p}_n,\mathbf{q}_1,\ldots,\mathbf{q}_m)|\mathbf{Q},\mathbf{q}_1,\ldots,\mathbf{q}_m\rangle\ , \tag{A7}$$

where the coefficients $\alpha(\mathbf{p}_1,\ldots,\mathbf{p}_n,\mathbf{q}_1,\ldots,\mathbf{q}_m)$ are obtained from the Schmidt and Löwdin transformations given in Ref. 26. The matrix element is

$$\begin{aligned}\langle\mathbf{P},\mathbf{p}_1,\ldots,\mathbf{p}_n|(H-E_0)|\mathbf{P}',\mathbf{p}'_1,\ldots,\mathbf{p}'_{n'}\rangle&=\sum_{\substack{m\le n\\ m'\le n'}}\sum_{\substack{\mathbf{q}_1\cdots\mathbf{q}_m\\ \mathbf{q}'_1\cdots\mathbf{q}'_{m'}}}\frac{1}{2m}\left[k^2-\mathbf{k}\cdot\left[\sum_{i=1,m}\mathbf{q}_i+\sum_{j=1,m'}\mathbf{q}'_j\right]\right]\\&\times\alpha^*(\mathbf{p}_1,\ldots,\mathbf{p}_n,\mathbf{q}_1,\ldots,\mathbf{q}_m)\alpha(\mathbf{p}'_1,\ldots,\mathbf{p}'_{n'},\mathbf{q}'_1,\ldots,\mathbf{q}'_{m'})\\&\times\langle\mathbf{Q},\mathbf{q}_1,\ldots,\mathbf{q}_m|\mathbf{Q}',\mathbf{q}'_1,\ldots,\mathbf{q}'_{m'}\rangle+\text{terms of order } k^0\ .\end{aligned} \tag{A8}$$

The coefficient of the $k^2$ term is just the overlap $\langle\mathbf{P},\mathbf{p}_1,\ldots,\mathbf{p}_n|\mathbf{P}',\mathbf{p}'_1,\ldots,\mathbf{p}'_{n'}\rangle$, which is zero for nondiagonal elements. Hence the leading term of $H'_{ij}$ is proportional to $k$ as asserted in Eq. (3.15).

## APPENDIX B: CALCULATION OF THE ONE- TO TWO-PHONON VERTEX

In order to calculate $\langle \mathbf{k}-l,l|H|\mathbf{k}\rangle$ matrix element we need to calculate the corresponding CB and PO matrix elements. Using Eqs. (A5) and (A6) we find

$$(\mathbf{k}-l,l|\mathbf{k})=\frac{1}{\sqrt{N}}\frac{S(l)-1}{\sqrt{S(l)}}\ , \tag{B1}$$

$$(\mathbf{k}-l,l|(H-E_0)|\mathbf{k})=\frac{1}{2m}(k^2-\mathbf{k}\cdot l)\frac{1}{\sqrt{N}}\frac{S(l)-1}{\sqrt{S(l)}}+O(k^0)\ , \tag{B2}$$

and the PO matrix element is given by [from here on we will omit the $O(k^0)$ terms]:

$$\begin{aligned}\{\mathbf{k}-l,l|(H-E_0)|\mathbf{k}\}&=(\mathbf{k}-l,l|(H-E_0)|\mathbf{k})\\&\quad-(\mathbf{k}-l,l|\mathbf{k})(\mathbf{k}|(H-E_0)|\mathbf{k})\\&=-\frac{1}{2m}\mathbf{k}\cdot l\frac{1}{\sqrt{N}}\frac{S(l)-1}{\sqrt{S(l)}}\\&\equiv-\frac{k}{m}\frac{1}{\sqrt{N}}\frac{\hat{\mathbf{k}}\cdot\hat{l}}{2}\sqrt{f_0(l)}\ .\end{aligned} \tag{B3}$$

The OCB states are obtained from PO states using the Lödwin transformation [Eq. (2.6)] for which the overlap of the two phonon PO states is needed. We first calculate the overlap of the two phonon CB states:

$$(\mathbf{k}-l,l|\mathbf{k}-\mathbf{m},\mathbf{m})=\frac{1}{N\sqrt{S(l)S(m)}}[S(|l-\mathbf{m}|)-1+\rho^3\int d^3r_i d^3r_j d^3r_k\, g_{ijk}\exp(-il\cdot\mathbf{r}_{ij}-i\mathbf{m}\cdot\mathbf{r}_{ik})]\ , \tag{B4}$$

where $g_{ijk}$ is the three-body distribution function. The three-body integral is calculated using the convolution approximation[15]

$$g_{ijk}=1+h_{ij}+h_{ik}+h_{jk}+h_{ij}h_{ik}+h_{ij}h_{jk}+h_{ik}h_{jk}+\rho\int d^3r_l\, h_{il}h_{jl}h_{kl}\ , \tag{B5}$$

where $h_{ij}=g(r_{ij})-1$. The result is

$$\begin{aligned}(\mathbf{k}-l,l|\mathbf{k}-\mathbf{m},\mathbf{m})&=\frac{1}{N\sqrt{S(l)S(m)}}\{S(|l-\mathbf{m}|)-1+[S(l)-1][S(m)-1]+[S(l)-1][S(|l-\mathbf{m}|)-1]\\&\quad+[S(m)-1][S(|l-\mathbf{m}|)-1]+[S(l)-1][S(m)-1][S(|l-\mathbf{m}|)-1]\}\\&=\frac{1}{N\sqrt{S(l)S(m)}}\{S(l)S(m)[S(|l-\mathbf{m}|)-1]+[S(l)-1][S(m)-1]\}\ .\end{aligned} \tag{B6}$$

From Eqs. (B1) and (B6) it follows that the overlap of the PO two-phonon states is given by

$$\begin{aligned}\{\mathbf{k}-l,l|\mathbf{k}-\mathbf{m},\mathbf{m}\}&=(\mathbf{k}-l,l|\mathbf{k}-\mathbf{m},\mathbf{m})-(\mathbf{k}-l,l|\mathbf{k})(\mathbf{k}|\mathbf{k}-\mathbf{m},\mathbf{m})\\&=\frac{1}{N}\sqrt{S(l)S(m)}[S(|l-\mathbf{m}|)-1]\ .\end{aligned} \tag{B7}$$

The one- to two-phonon OCB matrix element of the Hamiltonian can be calculated using PO matrix elements (B3) and (B7) and Eq. (2.6) as follows:

$$\begin{aligned}\langle \mathbf{k}-l,l|H|\mathbf{k}\rangle&=\{\mathbf{k}-l,l|(H-E_0)|\mathbf{k}\}-\frac{1}{2}\sum_{l_1}\overline{\{\mathbf{k}-l,l|\mathbf{k}-l_1,l_1\}}\{\mathbf{k}-l_1,l_1|(H-E_0)|\mathbf{k}\}\\&\quad+\frac{3}{8}\sum_{l_1,l_2}\overline{\{\mathbf{k}-l,l|\mathbf{k}-l_1,l_1\}\{\mathbf{k}-l_1,l_1|\mathbf{k}-l_2,l_2\}}\{\mathbf{k}-l_2,l_2|(H-E_0)|\mathbf{k}\}-\cdots\\&=-\frac{1}{\sqrt{N}}\frac{k}{2m}\left[\hat{\mathbf{k}}\cdot l\frac{S(l)-1}{\sqrt{S(l)}}-\frac{1}{2}\int\frac{d^3l_1}{(2\pi)^3\rho}\sqrt{S(l)S(l_1)}[S(|l-l_1|)-1]\hat{\mathbf{k}}\cdot l_1\frac{S(l_1)-1}{\sqrt{S(l_1)}}\right.\\&\quad+\frac{3}{8}\int\frac{d^3l_1}{(2\pi)^3\rho}\int\frac{d^3l_2}{(2\pi)^3\rho}\sqrt{S(l)S(l_1)}[S(|l-l_1|)-1]\\&\quad\left.\times\sqrt{S(l_1)S(l_2)}[S(|l_1-l_2|)-1]\hat{\mathbf{k}}\cdot l_2\frac{S(l_2)-1}{\sqrt{S(l_2)}}-\cdots\right]\\&=-\frac{1}{\sqrt{N}}\frac{k}{2m}\hat{\mathbf{k}}\cdot\hat{l}\left[\sqrt{f_0(l)}+\sqrt{S(l)}\left[-\frac{1}{2}\int\frac{d^3l_1}{(2\pi)^3\rho}A(l,l_1)l_1\frac{S(l_1)-1}{S(l_1)}\right.\right.\\&\quad\left.\left.+\frac{3}{8}\int\frac{d^3l_1}{(2\pi)^3\rho}A(l,l_1)\int\frac{d^3l_2}{(2\pi)^3\rho}A(l_1,l_2)l_2\frac{S(l_2)-1}{S(l_2)}-\cdots\right]\right]\end{aligned} \tag{B8}$$

$$\equiv-\frac{k}{m}\frac{1}{\sqrt{N}}\frac{\hat{\mathbf{k}}\cdot\hat{l}}{2}\sqrt{f(l)}\ , \tag{B9}$$

where

$$A(l,\mathbf{m})\equiv\hat{l}\cdot\hat{\mathbf{m}}S(m)[S(|l-\mathbf{m}|)-1]\ . \tag{B10}$$

When $l\to 0$ the function $A(l,l_1)$ can be expanded in $l$ and substituted in Eq. (B8). The angular integral of the zeroth-order term vanishes, and the large parentheses in Eq. (B8) is proportional to $l$. Thus, the function $f(l)$ is linear for small values of $l$ and has the same slope as $f_0(l)$. The functions $f(l)$ and $f_0(l)$ computed using experimental $S(l)$ for liquid $^4$He at low temperatures[28] are shown in Fig. 3.

We want to stress that the simple angular dependence of the one- to two-phonon matrix element (B9) and the linearity of the function $f(l)$, which are both crucial for the present calculation of the scaling function $J(y)$, are not artifacts of the convolution approximation that was used in calculation of the overlap of two-phonon PO states [Eq. (B7)], but rather a genuine property of the matrix element (B9). Indeed, the three-body integral in Eq. (B4) depends only on $l$, $m$ and $\hat{l}\cdot\hat{\mathbf{m}}$ due to the isotropy of the liquid, and so does the overlap (B7). This property alone fixes the angular dependence in Eq. (B9). An additional feature of the overlap (B7) is that it vanishes when $l\to 0$ or $m\to 0$ since PO states with an unequal number of phonons are mutually orthogonal by construction, which implies the linearity of the function $f(l)$ at the origin.

## APPENDIX C: PROOF OF EQ. (4.7)

The Ward identity

$$\hat{\mathbf{k}}\cdot l\Lambda(l,y)=\Sigma_S(y)-\Sigma_S(y+\hat{\mathbf{k}}\cdot l) \tag{C1}$$

establishes the connection between the proper self-energy $\Sigma_S(y)$ and the vertex correction $\Lambda(l,y)$. The diagrams that contribute to the $\Sigma_S(y)$ are shown in Fig. 2(a). If an external leg $l$ is attached to any hard phonon propagator in any of the $\Sigma_S(y)$ diagrams, a diagram contributing to the $\Lambda(l,y)$ is obtained. In fact, all the diagrams that contribute to the $\Lambda(l,y)$ [shown in Fig. 2(b)] can be generated in this way from the $\Sigma_S(y)$ diagrams. Thus, there is one-to-one correspondence between the diagrams that contribute to $\Sigma_S(y)$ and the groups of diagrams that contribute to the $\Lambda(l,y)$ that have the same arrangement of the internal lines as the $\Sigma_S(y)$ diagram plus an additional external leg $l$ attached to any hard phonon propagator. An example of this correspondence is shown in Fig. 5(a).

The $\Sigma_S(y)$ diagrams can be enumerated by an index $\nu$:

$$\Sigma_S(y)=\sum_\nu \Sigma_{S,\nu}(y)\ . \tag{C2}$$

The same enumeration scheme can be extended to the corresponding groups of the $\Lambda(1,y)$ diagrams:

$$\Lambda(l,y)=\sum_\nu \Lambda_\nu(l,y)\ , \tag{C3}$$

where the diagrams in the group $\Lambda_\nu$ can be generated from the diagram $\Sigma_\nu$ by a procedure discussed above. We will prove the Ward identity (C1) by showing that it

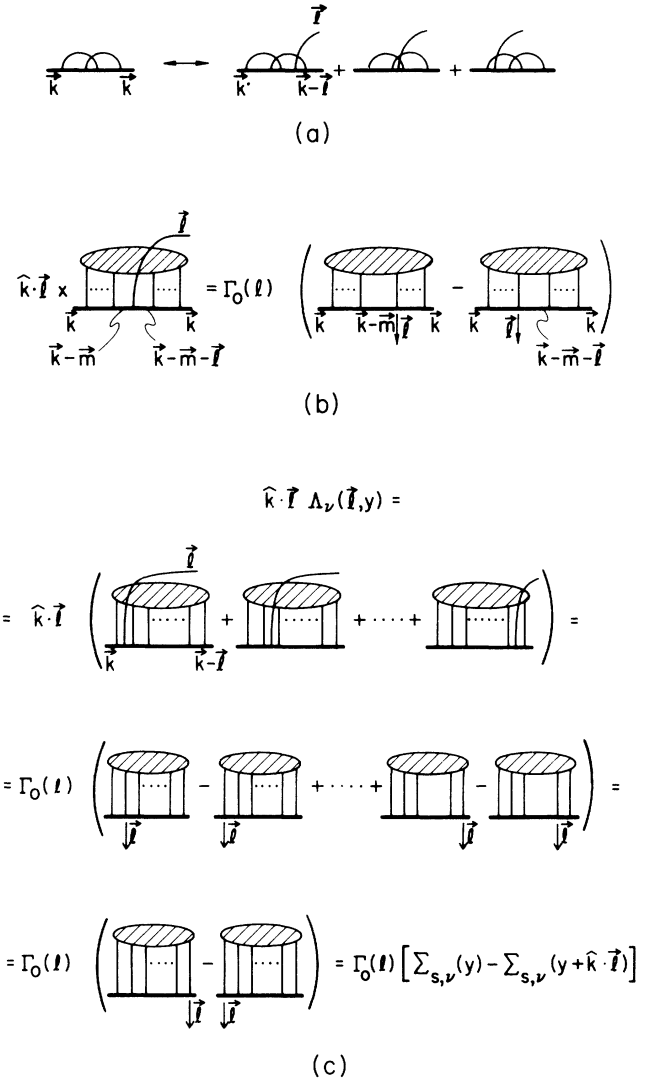


FIG. 5. The proof of the Ward identity [Eq. (4.7)]. (a) An example of the correspondence between $\Sigma_S(y)$ diagrams and groups of $\Lambda(l,y)$ diagrams. (b) Graphical representation of equation (C6). An arrow pointing from a vertex denotes an extraction of the momentum from the hard phonon propagator; shaded oval stands for an arbitrary complex connection scheme of the internal lines. (c) The proof of Eq. (C4).

holds for each group $\nu$ separately:

$$\hat{\mathbf{k}}\cdot l\Lambda_\nu(l,y)=\Sigma_{S,\nu}(y)-\Sigma_{S,\nu}(y+\hat{\mathbf{k}}\cdot l)\ ,\ \forall\nu\ . \tag{C4}$$

We begin the proof of Eq. (C4) by quoting the identity

$$\hat{\mathbf{k}}\cdot l[y+\hat{\mathbf{k}}\cdot\mathbf{m}+i\eta]^{-1}[y+\hat{\mathbf{k}}\cdot(\mathbf{m}+l)+i\eta]^{-1}$$
$$=[y+\hat{\mathbf{k}}\cdot\mathbf{m}+i\eta]^{-1}-[y+\hat{\mathbf{k}}\cdot(\mathbf{m}+l)+i\eta]^{-1}\ . \tag{C5}$$

From Eqs. (3.13), (3.14), (4.2), and (C5) it follows that

$$\hat{\mathbf{k}}\cdot lG_0(y+\hat{\mathbf{k}}\cdot\mathbf{m})\frac{m}{k}\Gamma_0(l)G_0[y+\hat{\mathbf{k}}\cdot(\mathbf{m}+l)]$$
$$=\Gamma_0(l)\{G_0(y+\mathbf{k}\cdot\mathbf{m})-G_0[y+\hat{\mathbf{k}}\cdot(\mathbf{m}+l)]\}\ . \tag{C6}$$

Equation (C6) has a simple graphical representation as is shown in Fig. 5(b). An arrow pointing from a vertex denotes an extraction of the momentum from the hard phonon propagator, which is an artifact of the removed external leg $l$. A shaded oval stands for an arbitrary complex connection scheme of the internal lines.

Next, we consider the arbitrary group $\Lambda_\nu$ of the diagrams contributing to the vertex correction $\Lambda(l,y)$. With the aid of Eq. (C6) it is easy to demonstrate that Eq. (C4) holds for an arbitrary $\nu$ as is done in Fig. 5(c). This finishes the proof of the Ward identity, since it was already shown that the validity of Eq. (C4) for all $\nu$'s implies Eq. (C1).


[1]P. Martel, E. C. Svensson, A. D. B. Woods, V. F. Sears, and R. A. Cowley, J. Low Temp. Phys. **23**, 285 (1976).

[2]A. D. B. Woods and V. F. Sears, Phys. Rev. Lett. **39**, 415 (1977).

[3]V. F. Sears, E. C. Svensson, P. Martel, and A. D. B. Woods, Phys. Rev. Lett. **49**, 415 (1982).

[4]H. A. Mook, Phys. Rev. Lett. **32**, 1167 (1974).

[5]H. A. Mook, Phys. Rev. Lett. **51**, 1454 (1983).

[6]H. R. Glyde and E. C. Svensson, in *Methods in Experimental Physics*, edited by D. L. Price and K. Skold (Academic, New York, 1987), Vol. 23, Part B.

[7]T. R. Sosnick, W. M. Snow, P. E. Sokol, and R. N. Silver, Europhys. Lett. **9**, 707 (1989).

[8]G. B. West, Phys. Rep. **18C**, 263 (1975).

[9]P. C. Hohenberg and P. M. Platzman, Phys. Rev. **152**, 198 (1966).

[10]L. J. Rodriguez, H. A. Gerch, and H. A. Mook, Phys. Rev. A **9**, 2085 (1974).

[11]R. N. Silver, Phys. Rev. B **38**, 2283 (1988).

[12]R. N. Silver, in *Momentum Distributions*, edited by R. N. Silver and P. E. Sokol (Plenum, New York, 1989).

[13]P. E. Sokol, in *Momentum Distributions*, edited by R. N. Silver and P. E. Sokol (Plenum, New York, 1989).

[14]C. Carraro and S. E. Koonin, Phys. Rev. Lett. **65**, 2792 (1990).

[15]E. Feenberg, *Theory of Quantum Liquids* (Academic, New York, 1969).

[16]V. F. Sears, Phys. Rev. **185**, 200 (1969).

[17]V. F. Sears, Phys. Rev. B **30**, 44 (1984).

[18]A. Belić and V. R. Pandharipande, Phys. Rev. B **39**, 2696 (1989).

[19]H. A. Gerch and L. J. Rodriguez, Phys. Rev. A **8**, 905 (1973).

[20]A. S. Rinat, Phys. Rev. B **40**, 6625 (1989).

[21]A. S. Rinat and M. F. Taragin, Phys. Rev. B **41**, 4247 (1990).

[22]J. J. Weinstein and J. W. Negele, Phys. Rev. Lett. **49**, 1016 (1982).

[23]E. Monousakis and V. R. Pandharipande, Phys. Rev. B **33**, 150 (1986).

[24]R. P. Feynman, Phys. Rev. **94**, 262 (1954).

[25]P. O. Löwdin, J. Chem. Phys. **18**, 365 (1950).

[26]S. Fantoni and V. R. Pandharipande, Phys. Rev. C **37**, 1697 (1988).

[27]M. J. Lighthill, *Introduction to Fourier Analysis and Generalised Functions* (Cambridge University, New York, 1959).

[28]H. N. Robkoff and R. B. Hallock, Phys. Rev. B **25**, 1572 (1982).

[29]E. Manousakis, V. R. Pandharipande, and Q. N. Usmani, Phys. Rev. B **31**, 7022 (1985); **43**, 13587 (1991).

[30]P. A. Whitlock, D. M. Ceperley, G. V. Chester, and M. H. Kalos, Phys. Rev. B **19**, 5598 (1979).